

A Skew Dividing Surface for Accurate Nonadiabatic Mean-Field Ring Polymer Rates

Britta A. Johnson¹ and Nandini Ananth^{1, a)}

Department of Chemistry and Biochemistry, Cornell University, Ithaca, New York 14850 U.S.A

(Dated: 28 February 2025)

Mean-Field Ring Polymer Molecular Dynamics (MF-RPMD) is a powerful, efficient, and accurate method for approximate quantum dynamic simulations of multi-level system dynamics. Although early efforts using MF-RPMD to compute nonadiabatic reaction rates failed, recent work showed that this can be remedied by including a simple, if *ad hoc*, correction term that accounts for the formation of ‘kinked’ or mixed electronic state ring polymer configurations. Here, we build on this idea to develop a rigorous MF-RPMD rate theory by introducing a novel reaction coordinate with a dividing surface that constrains nuclear positions to configurations where the reactant and product state potentials are near-degenerate *and* that samples kinked electronic state configurations. We demonstrate the numerical accuracy of this method in computing rates for a series of nonadiabatic model systems.

I. INTRODUCTION

Nonadiabatic condensed phase reactions play a critical role in understanding reaction mechanisms for a diverse range of interesting systems; these reactions range from proton coupled electron transfer in biological systems to charge transfer and fluorescence in energetic materials.^{1–6} The development of accurate and scalable theoretical methods for characterizing nonadiabatic energy and charge transfer remains an outstanding challenge.

A range of real-time dynamic methods including mixed quantum-classical^{7–10} and semiclassical methods^{11–19} have been used to simulate nonadiabatic reaction dynamics and compute rates; however, many of these methods cannot be easily scaled to the simulation of large condensed phase reactions. Path integral based methods like centroid-molecular dynamics^{20,21} and ring polymer molecular dynamics (RPMD)²² have shown particular promise in modeling condensed phase energy transfer reactions.^{23–29} These methods capture nuclear quantum effects like tunneling and zero-point energy while using only classical trajectories making them suitable for atomistic simulations of charge transfer in condensed phase systems. In particular, ring polymer molecular dynamics has been used to accurately calculate thermal rate constants for electron transfer (ET) in the normal and activationless regimes, and proton-coupled electron transfer.^{30–32} RPMD has also been extended to systems with coupled electronic states with the more successful formulations including mean-field (MF)-RPMD,³³ kinetically constrained (KC)-RPMD,^{32,34} nonadiabatic RPMD,³⁵ coherent-state RPMD,³⁶ and mapping-variable RPMD.^{37–40} KC-RPMD has been previously used to compute reaction rates for a model ET system in the normal and inverted Marcus regimes. Of the multi-state RPMD methods, MF-RPMD is uniquely efficient, relying on effective state-averaged

electronic forces to drive nuclear dynamics and requiring no additional variables making it suitable for large scale atomistic simulations. Here, we focus on developing a rigorous MF-RPMD rate theory that requires only real-time, classical, nuclear trajectories to compute nonadiabatic reaction rates.

Initial efforts to compute nonadiabatic reaction rates from MF-RPMD significantly overestimated the rate.^{32,41,42} Previously, one of us showed that this could be remedied by ensuring MF-RPMD trajectories sampled ‘kinked’ or mixed-electronic state ring polymer configurations at the dividing surface.⁴¹ Unfortunately, the *ad hoc* introduction of a constraint on the types of electronic state configurations sampled at the dividing surface resulted in an inconsistent flux-side formulation of the rate constant and a difficult-to-implement simulation protocol. We present a novel MF-RPMD reaction coordinate, the skew coordinate, that allows us to formulate a rigorous flux-side correlation function for the computation of nonadiabatic rates. We demonstrate the accuracy of this approach in a series of numerical simulations on model nonadiabatic ET systems over a wide range of driving forces.

This paper is organized as follows. In Section II we briefly review the MF-RPMD formalism, and introduce the new skew reaction coordinate. In section III we describe the model systems studied here and section IV outlines the details of the MF-RPMD rate calculation. In section V we numerically demonstrate sampling by the skew coordinate and present the results of our nonadiabatic rate calculations. We summarize our findings in section VI.

II. THEORY

A. Mean-Field Ring Polymer Molecular Dynamics

In this section we review MF-RPMD⁴¹. For a general K -level system with d nuclear degrees of freedom, the

^{a)}ananth@cornell.edu

diabatic Hamiltonian is

$$\hat{H} = \sum_{j=1}^d \frac{\hat{P}_j^2}{2M_j} + \sum_{n,m=1}^K |n\rangle V_{nm}(\hat{R}) \langle m|, \quad (1)$$

where \hat{R} and \hat{P} are d -dimensional nuclear position and momentum vector operators, respectively. The quantum partition function is discretized via repeated insertion of N copies of the identity to obtain

$$Z = \text{Tr}[e^{-\beta\hat{H}}] = \int d\{R_\alpha\} \sum_{\{n_\alpha\}=1}^K \prod_{\alpha=1}^N \langle R_\alpha, n_\alpha | e^{-\beta_N \hat{H}} | R_{\alpha+1}, n_{\alpha+1} \rangle, \quad (2)$$

where $\beta_N = 1/(Nk_B T)$, T is temperature, N is the number of imaginary time slices (or beads), and R_α, n_α refer to the nuclear position and electronic state of the α^{th} bead, respectively. In Eq. 2, we use a shorthand for the multi-dimensional integral over nuclear coordinates and summation over electronic states, $\int d\{R_\alpha\} = \int dR_1 \int dR_2 \dots \int dR_N$ and $\sum_{\{n_\alpha\}=1}^K = \sum_{n_1} \sum_{n_2} \dots \sum_{n_N}$. Evaluating the matrix elements using the Trotter and short-time approximations, we obtain,^{43,44}

$$Z \propto \lim_{N \rightarrow \infty} \int \{dR_\alpha\} e^{-\beta_N V_N(\{R_\alpha\})} \text{Tr}[\Gamma], \quad (3)$$

where

$$V_N = \sum_{j=1}^d \sum_{\alpha=1}^N \left[\frac{M_j}{2\beta_N^2} (R_{j,\alpha} - R_{j,\alpha+1})^2 \right], \quad (4)$$

$$\Gamma = \prod_{\alpha=1}^N M(R_\alpha), \quad (5)$$

and M is the $K \times K$ -dimensional matrix

$$M_{nm}(R_\alpha) = \begin{cases} e^{-\beta_N V_{nn}(R_\alpha)} & n = m \\ \beta_N V_{nm}(R_\alpha) e^{-\beta_N V_{nn}(R_\alpha)} & n \neq m \end{cases} \quad (6)$$

Finally, moving the trace in Eq. 3 into the exponential and introducing N normalized Gaussian integrals in nuclear momenta, we obtain a phase-space expression for the canonical partition function,

$$Z \propto \lim_{N \rightarrow \infty} \int \{dR_\alpha\} \int \{dP_\alpha\} e^{-\beta_N H_N(\{R_\alpha\}, \{P_\alpha\})}, \quad (7)$$

where the MF-RPMD Hamiltonian is

$$H_N = \sum_{j=1}^d \sum_{\alpha=1}^N \left[\frac{M_j}{2\beta_N^2} (R_{j,\alpha} - R_{j,\alpha+1})^2 + \frac{P_{j,\alpha}^2}{2M_j} \right] - \frac{1}{\beta_N} \ln(\text{Tr}[\Gamma]). \quad (8)$$

The MF-RPMD approximation to quantum real-time thermal correlation functions is obtained by sampling initial conditions from an exact quantum canonical ensemble and time-evolving trajectories under the MF-RPMD Hamiltonian in Eq. 8 with M_j chosen to the physical mass of the nuclei.

B. A Skew Dividing Surface for MF-RPMD rate theory

For a general reaction with a barrier, the rate constant can be written in terms of a flux-side correlation function^{43,45}.

$$k = \lim_{t \rightarrow \infty} \frac{\langle \delta(\xi_0 - \xi^\ddagger) \xi_0 h(\xi_t - \xi^\ddagger) \rangle}{\langle h(\xi^\ddagger - \xi_0) \rangle}, \quad (9)$$

where the angular brackets indicate a canonical ensemble average, δ is a delta function, and h is the Heaviside function. For a K -level system, the generalized reaction coordinate, ξ , may be a function of the nuclear $\{R\}$ and electronic state $\{n\}$ variables; ξ_0 is the initial value of this coordinate at time $t = 0$, ξ_t is the value at time t , and ξ^\ddagger is value at the dividing surface.

The MF-RPMD Hamiltonian in Eq. 8 is an explicit function of the nuclear positions and momenta, with the effective mean-field potential, Γ , obtained by tracing over all possible electronic state configurations. Previous attempts to calculate nonadiabatic reaction rates using MF-RPMD relied on a nuclear centroid based definition of the dividing surface, $\delta(\bar{R} - R^\ddagger)$, where the reaction coordinate is the centroid, $\bar{R} = \frac{1}{N} \sum_{\alpha} R_\alpha$, and R^\ddagger represents the nuclear configuration at which the two diabatic electronic state potentials cross. It was shown that MF-RPMD rates computed with this centroid based reaction coordinate were accurate for adiabatic systems, but significantly overestimated the rate for nonadiabatic systems.³⁴ One of us previously showed that the low probability of sampling ‘kinked’ or multi-electronic state ring polymer configurations for nonadiabatic process even at the nuclear centroid dividing surface was responsible for the failure of MF-RPMD.⁴¹ Further, it was established that a dividing surface obtained by sampling only kinked configurations *and* constraining the nuclear centroid position resulted in accurate MF-RPMD rates for a range of nonadiabatic model systems.⁴¹ However, the mismatch between reaction coordinate and the *ad hoc* dividing surface resulted in a inconsistent flux-side correlation function that was challenging to implement in both the normal and inverted Marcus regimes. Here, we propose an improved MF-RPMD rate theory by introducing a new ‘skew’ reaction coordinate. We show that constraining to the corresponding dividing surface results in kinked ring polymer configurations in the vicinity of R^\ddagger without any additional constraints.

We start by recognizing that the average electronic force on the nuclear degrees of freedom is due to the mean-field potential, $\Gamma(\{R_\alpha\})$ in Eq. 5 that is an average over all possible electronic state configurations. This allows us to divide the contributions to Γ into two types, all ‘reactant’-like configurations $\Gamma_r(\{R_\alpha\}) = \sum_{k=N^\ddagger}^N \Gamma_k(\{R_\alpha\})$ and all ‘product’-like configurations into the function $\Gamma_p(\{R_\alpha\}) = \sum_{k=0}^{N^\ddagger} \Gamma_k(\{R_\alpha\})$ where

$$\Gamma_k = \prod_{\alpha=1}^{N-k} M(R_\alpha) \mathbb{P}_2 \prod_{\alpha=N-k+1}^N M(R_\alpha) \mathbb{P}_1, \quad (10)$$

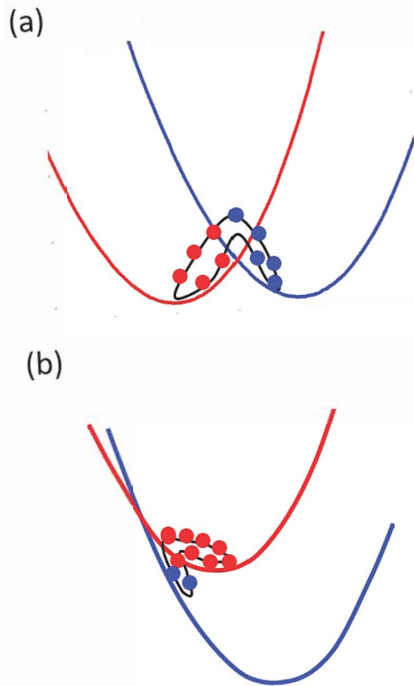


FIG. 1. (a) Shows a symmetric two-level system where half the RP beads are in the reactant state (red) and the other half are in the product state (blue). As the reactant state is destabilized and the driving force increases, we find that constraining nuclear RP configurations to the vicinity of the diabatic crossing can be achieved by increasing the number of beads in the reactant state as shown in (b).

and \mathbb{P}_i is the projection operator onto state i . Physically, Eq. 10 is representative of MF-RP configurations where the last k beads are in electronic state 1 and the remaining $N - k$ beads are in state 2. The value of N^\ddagger in the expression for Γ_r and Γ_p is determined based on the driving force; as the driving force increases, N^\ddagger also increases as shown in the cartoon Fig. 1. We note that this idea is in keeping with studies of the MF-RP instanton for multistate systems that has an increasing number of RP beads in the reactant state as we move from the Marcus normal regime to the inverted regime.⁴⁶

The numerical choice of N^\ddagger is best made by generating histograms of the nuclear configurations sampled by the MF-RPMD potential where the mean-field potential, Γ , is replaced by Γ_{N^\ddagger} . We find that for a small range of N^\ddagger we see significant sampling at R^\ddagger , the nuclear configuration at which the two diabatic potentials cross. This suggests that defining a dividing surface of the form $\delta(\Gamma - \Gamma_{N^\ddagger})$ will allow us to sample kinked configurations while also constraining nuclear RP configurations to the vicinity crossing, thereby removing the need for an artificial double constraint such as was previously used.

We define our reaction coordinate as,

$$\xi = \Gamma_p - \Gamma_r, \quad (11)$$

where Γ_p and Γ_r have been previously defined as the po-

tential terms corresponding to product-like and reactant-like MF-RP configurations. We can then characterize the progress of the reaction along this reaction coordinate:

$$\begin{aligned} \xi < 0 & \text{ in the reactant well} \\ \xi = 0 & \text{ at the transition state} \\ \xi > 0 & \text{ in the product well.} \end{aligned}$$

Substituting this definition of the reaction coordinate in the flux-side expression for the rate we obtain,

$$k = \lim_{t \rightarrow \infty} \frac{\int d\{R_\alpha, P_\alpha\} e^{-\beta_N H_N} \delta(\xi(0)) \dot{\xi}(0) h(\xi(t))}{\int d\{R_\alpha, P_\alpha\} e^{-\beta_N H_N} h(\xi(0))}. \quad (12)$$

Implementing the constraint, $\delta(\Gamma_p(0) - \Gamma_r(0))$, in Eq. 12 can be challenging; however, we recognize that, in general, $\Gamma_r = \Gamma_p$ only when $\Gamma_r = \Gamma_p = \Gamma_{N^\ddagger}$, and therefore, following our earlier definition of the MF-RP potential, we have $\Gamma = \Gamma_r + \Gamma_p - \Gamma_{N^\ddagger} = \Gamma_{N^\ddagger}$. This allows us to replace the delta function in the numerator of Eq. 12 by an equivalent function, $\delta(\Gamma(0) - \Gamma_{N^\ddagger})$ to obtain a simplified MF-RP rate expression,

$$k = \lim_{t \rightarrow \infty} \frac{\int d\{R_\alpha, P_\alpha\} e^{-\beta_N H_N} \text{Tr}[\Gamma_{N^\ddagger}] \dot{\xi}(0) h(\xi(t))}{\int d\{R_\alpha, P_\alpha\} e^{-\beta_N H_N} h(\xi(0))}. \quad (13)$$

Further, we recognize that the largest contributions to Γ_r and Γ_p are from configurations where all the beads are in the same electronic state. This allows us to write $\Gamma_p - \Gamma_r \equiv \Gamma_0 - \Gamma_N$. Finally, we note that the reactant partition function can be equivalently computed by simply tracing over all nuclear configurations where the beads are in the reactant state. Putting all this together, we arrive at a final expression for the rate

$$k = \lim_{t \rightarrow \infty} \frac{\int d\{R_\alpha, P_\alpha\} e^{-\beta_N H_N^0} \text{Tr}[\Gamma_{N^\ddagger}] \Delta \dot{\Gamma}(0) h(\Delta \Gamma(t))}{\int d\{R_\alpha, P_\alpha\} e^{-\beta_N H_N^0} \text{Tr}[\Gamma_N(0)]}, \quad (14)$$

where $\Delta \Gamma = \Gamma_N - \Gamma_0$, and H_N^0 is the free ring polymer Hamiltonian that includes only terms on the first line of Eq. 8

C. Nonadiabatic Rate Theories

The Marcus theory (MT) rate for a nonadiabatic electron transfer reaction with a classical solvent is,⁴⁷

$$k_{\text{MT}} = \frac{2\pi}{\hbar} |V_{nm}|^2 \sqrt{\frac{\beta}{4\pi\lambda}} e^{-\beta(\lambda - \epsilon)^2/4\lambda}, \quad (15)$$

where λ is the reorganization energy, ϵ is the driving force, and V_{nm} is the diabatic coupling between the reactant and product electronic states.

Fermi's golden rule rate theory for a nonadiabatic electron transfer system where the reactant and product state potential energy surfaces are displaced harmonic

oscillators with frequency ω_s and with a quantized solvent take the simple analytical form^{48,49}

$$k_{\text{FGR}} = \frac{2\pi}{\hbar\omega_s} |\Delta|^2 e^{vz - S \coth(z)} I_v(S \operatorname{csch}(z)), \quad (16)$$

where $z = \beta\omega_s/2$, $v = \epsilon/\omega_s$, $S = M_s\omega_s V_d^2/2\hbar$, M_s is the solvent mass, I_v is a modified Bessel function of the first kind, and V_d is the horizontal displacement of the diabatic potential energy surfaces.

III. MODEL SYSTEM

We calculate the rates for a model condensed-phase ET system with a potential

$$V(\hat{R}) = V_S(\hat{s}) + V_B(\hat{R}) \quad (17)$$

where the configuration vector $\hat{R} = \{\hat{s}, \hat{Q}\}$ represents the solvent polarization coordinate, s , and the bath coordinates, Q . The diabatic potential energy matrix is

$$V_S(\hat{s}) = \begin{pmatrix} V_{11}(\hat{s}) & \Delta \\ \Delta & V_{22}(\hat{s}) \end{pmatrix}, \quad (18)$$

where the diagonal elements are $V_{11}(\hat{s}) = A\hat{s}^2 + B\hat{s} + \epsilon$, $V_{22}(\hat{s}) = A\hat{s}^2 - B\hat{s}$, the driving force is represented by ϵ , and the diabatic coupling a constant, Δ . The solvent coordinate is linearly coupled to a thermal bath of f harmonic oscillators,

$$V_B(\hat{R}) = \sum_{j=1}^f \left[\frac{1}{2} M_B \omega_j^2 \left(\hat{Q}_j - \frac{c_j \hat{s}}{M_B \omega_j^2} \right)^2 \right] \quad (19)$$

where M_S and M_B are the solvent and bath mass respectively. The bath is described by an Ohmic spectral density

$$J(\omega) = \eta \omega e^{-\frac{\omega}{\omega_c}} \quad (20)$$

where ω_c is the cutoff frequency and η is the dimensionless friction coefficient. The spectral density is discretized into f oscillators²³

$$\omega_j = -\omega_c \ln \left(\frac{j - 0.5}{f} \right) \quad (21)$$

with coupled strengths

$$c_j = \omega_j \left(\frac{2\eta M_B \omega_c}{f\pi} \right)^{1/2} \quad (22)$$

The ET model parameters are shown in Table I.

IV. SIMULATION DETAILS

The rate expression in Eq. 13 may still be challenging to implement since the numerator requires sampling an

Parameters	Value
A	4.772×10^{-3}
B	2.288×10^{-2}
ϵ	$0.0 - 0.2366$
Δ	6.69×10^{-7}
M_S	1836.0
M_B	1836.0
f	12
ω_c	2.28×10^{-3}
$\eta/M_B\omega_c$	1.0
T	300 K

TABLE I. ET model parameters given in atomic units unless otherwise indicated.

ensemble constrained to our skew dividing surface while the denominator requires efficient sampling of the reactant region. To ensure proper sampling of all important regions of configuration space, we introduce an identity in the form of an integral over all possible nuclear RP centroid configurations to obtain

$$k = \lim_{t \rightarrow \infty} \frac{\int ds' \langle \Gamma_{N^\ddagger} \dot{\Delta}\Gamma(0) h(\Delta\Gamma(t)) \rangle_w}{\int ds' \langle \Gamma_N \rangle_w} \quad (23)$$

where $\langle \dots \rangle_w$ is used to indicate a phase space ensemble average over the nuclear bead configurations obtained by importance sampling from the distribution

$$w = e^{-\beta_N H_N^0(\{R_\alpha, P_\alpha\})} \delta(\bar{s} - s'). \quad (24)$$

The numerator and denominator are evaluated using a standard Metropolis algorithm to sample free RP configurations from $e^{-\beta_N H_N^0(\{R_\alpha, P_\alpha\})}$ in each window. We then impose the constraint by shifting the solvent RP centroid to \bar{s} to the s' value associated with each window. By scrolling through all possible nuclear RP centroid configurations, we ensure that the numerator and the denominator are sampled adequately. The integral over s' is evaluated using the trapezoid rule.

We establish the mean-field path integral converges with $N = 32$ beads for all simulations presented here. Importance sampling is performed in each window using 11000 decorrelated Monte Carlo steps, and the final 10000 configurations are used as initial conditions for trajectories evolved under the MF-RPMD Hamiltonian in equation 8 with a timestep of 0.05 a.u. The average initial velocity, $\dot{\Delta}\Gamma(0)$ is obtained by averaging over the finite difference derivative of $\Delta\Gamma$ calculated for three small intervals of time, $\Delta t = 5, 7, 10$ a.u. The integral over the solvent centroid configurations is performed over 150 windows evenly spaced between $s = -4.5$ and $s = +1.5$ for Models I-VIII. Model IX simulations are performed with 150 evenly spaced points between $s = -6.5$ and $s = -0.5$.

1. A Modified Implementation in the Inverted Regime

Physically, the probability of forming kinked configurations, where neighboring beads of the ring polymer are in different electronic states, depends on both the magnitude of the off-diagonal diabatic coupling and the energy gap between the reactant and product states. In the normal regime, we find that the kink probabilities computed using the MF-RP potential, $\Gamma(\{R_\alpha\})$ in Eq. 5 with the interaction matrix defined in Eq. 6, do indeed show a decreased probability at nuclear configurations where the energetic gap between reactant and product states is large. However, in the inverted regime, we see a breakdown of this: specifically, we find that in regions where the product state is much more favorable than the reactant state, the Boltzmann weight of beads in the product state is numerically larger than the penalty associated with kink formation resulting in an unphysically large probability of kink formation in regions where the reactant and product are energetically very different.

We correct for this by a simple modification of the nuclear interaction matrix in Eq. 6 that is used in computing Γ_{N^\ddagger} . Specifically, we replace V_{22} by $V_{11} + |V_{22} - V_{11}|$ in the appropriate off-diagonal term of the interaction matrix. This ensures that the energetic penalty associated with kink formation is correctly captured, since the value now depends only on the magnitude of the energy gap between states. Note that this is only used in the calculation of Γ_{N^\ddagger} ; dynamics are performed using the MF-RPMD Hamiltonian and the remaining terms in Eq. 23 are unaffected by this change.

V. RESULTS AND DISCUSSION

We present the results of our rate calculations for nine model systems that differ only in the driving force, ε , values; six of these systems (Models I-VI) are located in the normal regime and three (Models VII-IX) are in the inverted regime. To select the N^\ddagger values for each model, we look at the values for $\Gamma_k(\{R_\alpha\})$ for individual beads as a function of nuclear position.

Figure 2 shows a sample of the Γ_k curves for a model in the normal regime (Models III) and one inverted regime model (Model VIII). For each model, we find that there is a range of k values where Γ_k is maximized near the crossing (denoted s^\ddagger in the figure), the point where the reactant and product state are degenerate. We note that the inverted regime Γ_k is modified as described in the simulation details; we find that $N^\ddagger = 31$ is necessary to ensure that the dividing surface includes nuclear configurations to the left of the reactant minimum towards the diabatic crossing. For each model in the normal regime, we select an N^\ddagger value such that Γ_{N^\ddagger} peaks close to the crossing; the specific values we use are listed in Table II, and we note that the rates are relatively robust to this choice as long as the N^\ddagger values used sufficiently samples nuclear configurations in the vicinity of the diabatic

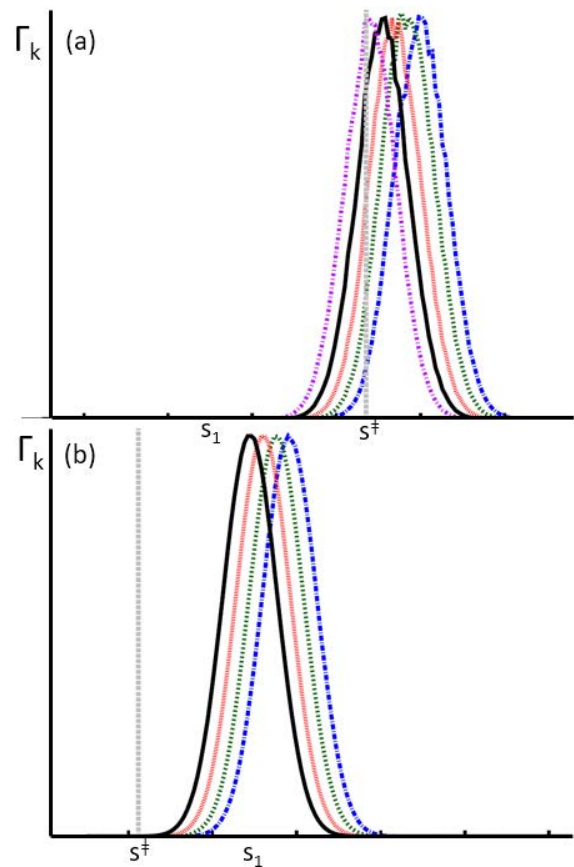


FIG. 2. Plots of the Γ_k functions for (a) model III and (b) model VIII. In both figures, the location of the diabatic crossing is designated by a dotted line at s^\ddagger , the reactant minimum indicated by s_1 , and Γ_k with $k = N^\ddagger$ is plotted as a black solid line. (a) For model III, Γ_k with $k = 16$ is shown in blue, $k = 17$ is in dark green, $k = 18$ is in red, $k = 19$ is in black, and $k = 20$ is in magenta. (b) For model VIII, Γ_k with $k = 28$ is shown in blue, $k = 29$ in dark green, $k = 30$ in red, and $k = 31$ in black.

crossing.

We present the MF-RPMD rate results in Fig. 3 and tabulate the corresponding values in Table. II. We find that the new reaction coordinate performs remarkably well in the normal regime, yielding results that are in quantitative agreement with Fermi Golden Rule rates for all six model systems. In the inverted regime, we find good agreement with Marcus theory rates rather than the golden rule rates. This initially surprising result can be attributed to the modified form of the interaction matrix we use. By making the kink probabilities strongly dependent on the energy gap, we increase the penalty at nuclear configurations where one may reasonably expect to see tunneling effects. As such, we find that the contribution to the overall rate is dominated by windows where the solvent centroid is constrained to the immediate vicinity of the diabatic crossing, yielding Marcus rates rather than FGR rates.

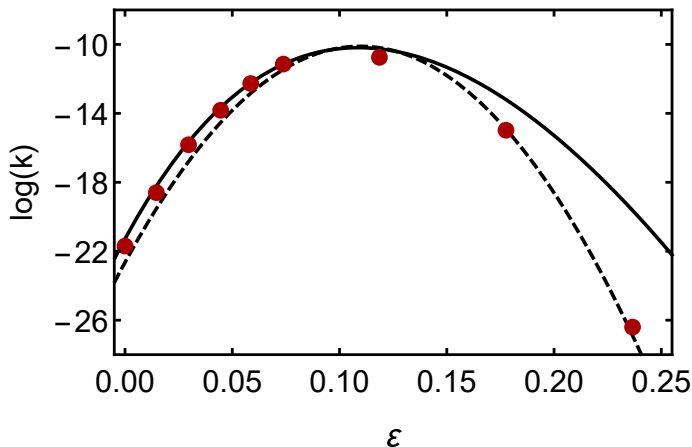


FIG. 3. ET rates for models I-IX. MF-RPMD rates with the skew reaction coordinate are shown as red circles, error bars are within the symbol size. The Fermi's Golden rule rates lie along the solid black line and the Marcus theory rates lie along the dashed line

Model	ϵ	N^\ddagger	$\log(k_{\text{MT}})$	$\log(k_{\text{MF}})$	$\log(k_{\text{FGR}})$
I	0.00	16	-22.65	-21.7	-21.28
II	0.0146	17	-19.53	-18.6	-18.23
III	0.0296	19	-16.79	-15.82	-15.66
IV	0.0446	21	-14.52	-13.82	-13.65
V	0.0586	23	-12.83	-12.27	-12.23
VI	0.0738	25	-11.45	-11.14	-11.15
VII	0.1186	29	-10.19	-10.75	-10.26
VIII	0.1776	31	-14.91	-14.98	-13.20
IX	0.2366	31	-26.89	-26.4	-19.63

TABLE II. ET rates for a range of driving forces. We report the N^\ddagger value used for each model, the corresponding Marcus theory rates (k_{MT}), MF-RPMD rates (k_{MF}), and Fermi Golden Rule rates (k_{FGR}) for each model. We see that the MF-RPMD rates are in near-perfect agreement with FGR rates in the normal regime and agree equally well with MT rates in the inverted regimes. All rate constants are in atomic units

VI. CONCLUSION

We demonstrate that the skew reaction coordinate introduced here can be used to obtain a rigorous MF-RPMD rate theory that is quantitatively accurate for the computation of nonadiabatic reaction rates in a wide range of model systems. MF-RPMD is the most efficient and easy to implement of the RPMD-based methods developed to simulate multi-state system dynamics, and this skew coordinate enables the use of this technique in simulations of nonadiabatic processes. The form of the reaction coordinate is general and requires only an understanding of the driving force regime for a particular reaction (information that is typically known even for complex systems) placing atomistic multi-state simulations within reach.

VII. ACKNOWLEDGEMENTS

This work was primarily supported by the U.S. Department of Energy, Office of Basic Energy Sciences, Division of Chemical Sciences, Geosciences and Biosciences through the Nanoporous Materials Genome Center under award numbers DE-FG02-17ER16362. Additionally, N. A. acknowledges support from the National Science Foundation Career Award Number CHE1555205.

VIII. DATA AVAILABILITY

The data that support the findings of this study are available from the corresponding author upon reasonable request.

- ¹R. Marcus and N. Sutin, *Biochimica et Biophysica Acta (BBA) - Reviews on Bioenergetics* **811**, 265 (1985).
- ²H. B. Gray and J. R. Winkler, *Annual Review of Biochemistry* **65**, 537 (1996), pMID: 8811189, <https://doi.org/10.1146/annurev.bi.65.070196.002541>.
- ³S. S. Skourtis, D. H. Waldeck, and D. N. Beratan, *Annual Review of Physical Chemistry* **61**, 461 (2010), pMID: 20192814, <https://doi.org/10.1146/annurev.physchem.012809.103436>.
- ⁴M. Azzouzi, J. Yan, T. Kirchartz, K. Liu, J. Wang, H. Wu, and J. Nelson, *Phys. Rev. X* **8**, 031055 (2018).
- ⁵D. R. Yarkony, *Chemical Reviews* **112**, 481 (2012), pMID: 22050109, <https://doi.org/10.1021/cr2001299>.
- ⁶S. Hammes-Schiffer and A. V. Soudackov, *The Journal of Physical Chemistry B* **112**, 14108 (2008), pMID: 18842015, <https://doi.org/10.1021/jp805876e>.
- ⁷J. C. Tully, *The Journal of Chemical Physics* **93**, 1061 (1990), <https://doi.org/10.1063/1.459170>.
- ⁸R. Kapral, *Annual Review of Physical Chemistry* **57**, 129 (2006), pMID: 16599807, <https://doi.org/10.1146/annurev.physchem.57.032905.104702>.
- ⁹A. Jain and J. E. Subotnik, *The Journal of Chemical Physics* **143**, 134107 (2015), <https://aip.scitation.org/doi/pdf/10.1063/1.4930549>.
- ¹⁰R. Crespo-Otero and M. Barbatti, *Chemical Reviews* **118**, 7026 (2018), pMID: 29767966, <https://doi.org/10.1021/acs.chemrev.7b00577>.
- ¹¹J. Cao and G. A. Voth, *The Journal of Chemical Physics* **106**, 1769 (1997), <https://doi.org/10.1063/1.474123>.
- ¹²J. Cao, C. Minichino, and G. A. Voth, *The Journal of Chemical Physics* **103**, 1391 (1995), <https://doi.org/10.1063/1.469762>.
- ¹³W. H. Miller and S. J. Cotton, *Faraday Discuss.* **195**, 9 (2016).
- ¹⁴S. J. Cotton and W. H. Miller, *The Journal of Physical Chemistry A* **117**, 7190 (2013), pMID: 23432081, <https://doi.org/10.1021/jp401078u>.
- ¹⁵J. O. Richardson, R. Bauer, and M. Thoss, *The Journal of Chemical Physics* **143**, 134115 (2015), <https://aip.scitation.org/doi/pdf/10.1063/1.4932361>.
- ¹⁶J. O. Richardson, *The Journal of Chemical Physics* **143**, 134116 (2015), <https://aip.scitation.org/doi/pdf/10.1063/1.4932362>.
- ¹⁷M. K. Lee, P. Huo, and D. F. Coker, *Annual Review of Physical Chemistry* **67**, 639 (2016), pMID: 27090842, <https://doi.org/10.1146/annurev-physchem-040215-112252>.
- ¹⁸N. Ananth, C. Venkataraman, and W. H. Miller, *The Journal of Chemical Physics* **127**, 084114 (2007), <https://doi.org/10.1063/1.2759932>.
- ¹⁹M. S. Church, T. J. H. Hele, G. S. Ezra, and N. Ananth, *The Journal of Chemical Physics* **148**, 102326 (2018), <https://doi.org/10.1063/1.5005557>.
- ²⁰J. Cao and G. A. Voth, *The Journal of Chemical Physics* **100**, 5106 (1994), <https://doi.org/10.1063/1.467176>.

- ²¹S. Jang and G. A. Voth, *The Journal of Chemical Physics* **111**, 2371 (1999), <https://doi.org/10.1063/1.479515>.
- ²²I. R. Craig and D. E. Manolopoulos, *The Journal of Chemical Physics* **121**, 3368 (2004), <https://doi.org/10.1063/1.1777575>.
- ²³I. R. Craig and D. E. Manolopoulos, *The Journal of Chemical Physics* **122**, 084106 (2005), <https://doi.org/10.1063/1.1850093>.
- ²⁴J. E. Lawrence and D. E. Manolopoulos, *Faraday Discuss.* **221**, 9 (2020).
- ²⁵I. S. Novikov, Y. V. Suleimanov, and A. V. Shapeev, *Phys. Chem. Chem. Phys.* **20**, 29503 (2018).
- ²⁶T. J. H. Hele and S. C. Althorpe, *The Journal of Chemical Physics* **138**, 084108 (2013), <https://doi.org/10.1063/1.4792697>.
- ²⁷S. C. Althorpe and T. J. H. Hele, *The Journal of Chemical Physics* **139**, 084115 (2013), <https://doi.org/10.1063/1.4819076>.
- ²⁸T. J. H. Hele and S. C. Althorpe, *The Journal of Chemical Physics* **144**, 174107 (2016), <https://doi.org/10.1063/1.4947589>.
- ²⁹S. Habershon, D. E. Manolopoulos, T. E. Markland, and T. F. Miller, *Annual Review of Physical Chemistry* **64**, 387 (2013), pMID: 23298242, <https://doi.org/10.1146/annurev-physchem-040412-110122>.
- ³⁰A. R. Menzelev, N. Ananth, and T. F. Miller, *The Journal of Chemical Physics* **135**, 074106 (2011), <https://doi.org/10.1063/1.3624766>.
- ³¹D. M. Wilkins, D. E. Manolopoulos, and L. X. Dang, *The Journal of Chemical Physics* **142**, 064509 (2015), <https://doi.org/10.1063/1.4907554>.
- ³²J. S. Kretchmer and T. F. Miller III, *Faraday Discuss.* **195**, 191 (2016).
- ³³Mean field RPMD has been used previously by many including D. E. Manolopoulos, T. F. Miller III, N. Ananth, J. C. Tully and I. R. Craig to evaluate nonadiabatic PI methods.
- ³⁴A. R. Menzelev, F. Bell, and T. F. Miller, *The Journal of Chemical Physics* **140**, 064103 (2014), <https://doi.org/10.1063/1.4863919>.
- ³⁵J. O. Richardson and M. Thoss, *The Journal of Chemical Physics* **139**, 031102 (2013), <https://doi.org/10.1063/1.4816124>.
- ³⁶S. N. Chowdhury and P. Huo, *The Journal of Chemical Physics* **147**, 214109 (2017), <https://doi.org/10.1063/1.4995616>.
- ³⁷N. Ananth and T. F. Miller, *The Journal of Chemical Physics* **133**, 234103 (2010), <https://doi.org/10.1063/1.3511700>.
- ³⁸N. Ananth, *The Journal of Chemical Physics* **139**, 124102 (2013), <https://doi.org/10.1063/1.4821590>.
- ³⁹J. R. Duke and N. Ananth, *The Journal of Physical Chemistry Letters* **6**, 4219 (2015), pMID: 26722962, <https://doi.org/10.1021/acs.jpcclett.5b01957>.
- ⁴⁰S. Pierre, J. R. Duke, T. J. H. Hele, and N. Ananth, *The Journal of Chemical Physics* **147**, 234103 (2017), <https://doi.org/10.1063/1.4986517>.
- ⁴¹J. R. Duke and N. Ananth, *Faraday Discuss.* **195**, 253 (2016).
- ⁴²T. J. H. Hele, “An electronically non-adiabatic generalization of ring polymer molecular dynamics,” (2013), arXiv:1308.3950 [physics.chem-ph].
- ⁴³D. Chandler, *Introduction to Modern Statistical Mechanics* (Oxford University Press, New York, 1987).
- ⁴⁴H. F. Trotter, *Proceedings of the American Mathematical Society* **10**, 545 (1959).
- ⁴⁵W. H. Miller, S. D. Schwartz, and J. W. Tromp, *The Journal of Chemical Physics* **79**, 4889 (1983), <https://doi.org/10.1063/1.445581>.
- ⁴⁶S. Ranya and N. Ananth, *The Journal of Chemical Physics* **152**, 114112 (2020), <https://doi.org/10.1063/1.5132807>.
- ⁴⁷R. A. Marcus and N. Sutin, *Biochim. Biophys. Acta* **811**, 265 (1985).
- ⁴⁸J. Ulstrup and J. Jortner, *J. Chem. Phys.* **63**, 4358 (1975).
- ⁴⁹J. Ulstrup, *Charge Transfer Processes in Condensed Media* (Springer Verlag, Berlin, 1979).